Microchimica Acta (2022) 189: 357
https://doi.org/10.1007/s00604-022-05455-7

ORIGINAL PAPER

Sensitive colorimetric detection of miRNA-155 via G-quadruplex DNAzyme decorated spherical nucleic acid

Kosar Shahsavar[1] · Ehsan Shokri[2] · Morteza Hosseini[1]

Received: 8 November 2021 / Accepted: 9 August 2022 / Published online: 30 August 2022

Abstract

Rapid and sensitive detection of biomarkers enables monitoring patients' health status and can enhance the early diagnosis of deadly diseases. In this work, we have developed a new colorimetric platform based on spherical nucleic acid (SNA) and G-quadruplex DNAzymes for the identification of specific miRNAs. The simple hybridization between the target miRNA and two capture probes (capture probe 1 located at AuNP surface and free capture probe 2) is the working principle of this biosensor. The hybridization and duplex formation among probes and miRNAs led to a significant decrease in the intensity of color change. A linear relationship between the decrease of colorimetric signal and the amount of target molecules was witnessed from 1 to 100 nM for miRNA-155. Using this method, we were able to detect concentrations of miRNA-155 as low as 0.7 nM. Furthermore, the proposed sensing platform can be utilized profitably to detect miRNA-155 in real human serum samples. We further investigated the applicability of the proposed method in a microfluidic system which displayed promising results.

Keywords Biosensor · Spherical nucleic acid · G-quadruplex DNAzyme · Colorimetry · miRNA-155

Introduction

As one of the leading causes of death, cancer horribly threatens human health, and therefore, its diagnosis and therapy have attracted growing attention in past years [1]. Biomarkers can be used to detect cancer disease in an early stage. microRNAs, the noninvasive biomarkers, are small single-stranded non-coding RNA and have different applications in cellular events, diagnosis of diseases, and monitoring treatment responses [2–4]. It has been shown that the aberrant expression of miRNA is related to all types of cancers [5–9]. Therefore, highly sensitive detection of miRNA is a great significance for the early diagnosis of cancer. Upregulation of miRNA-155 has been involved in several human malignancies, including B-cell lymphoma and lung and breast cancer [10]. miRNA-155 plays a role as an oncomir and promotes tumor development while negatively inhibiting tumor suppressor genes that control cell differentiation or apoptosis [11]. As a result, miRNA-155 is considered a potential diagnostic biomarker for certain diseases, including cancer.

Besides commonly used detection methods like Northern blotting, in situ hybridization (ISH), and reverse transcriptase polymerase chain reaction (RT-PCR), miRNA detection remains unattained because miRNAs are very short in length and present at low levels in a given sample [12, 13].

With the emergence of nanotechnology, versatile nanoplatforms have been developed that allow highly sensitive miRNA sensing [14–16].

Mirkin et al. introduced a method for preparing spherical nucleic acid (SNA), nanoparticles with a thick and oriented layer of nucleic acids covalently attached to their surfaces. SNA has a brunch of applications in molecular diagnostic, therapeutic, and material science due to its properties like high thermal stability, resistance to nuclease degradation, and minimal immune response [17]. It is worth mentioning that these features derive from a dense nucleic acid layer rather than cores [18]. The use of nucleic acid

✉ Morteza Hosseini
smhosseini@khayam.ut.ac.ir

[1] Nanobiosensors Lab, Department of Life Science Engineering, Faculty of New Sciences & Technologies, University of Tehran, Tehran, Iran

[2] Department of Nanotechnology, Agricultural Biotechnology Research Institute of Iran (ABRII), Agricultural Research, Education and Extension Organization (AREEO), Karaj, Iran

enzymes (DNAzyme) to produce a dense layer of nucleic acid on nanoparticles leads to the construction of specific SNAs serving as an ideal catalytic label. These SNAs that fabricate with DNAzymes are SNA enzymes (SNAzyme) [19]. Despite the different core structures (Au, Ag, Fe_3O_4, semiconductor quantum dots, silica, polymers, and etc.), the most widely studied SNA consists of gold nanoparticles (AuNPs) [20–23]. Au NPs have become favorable candidates for being core material because they can be functionalized with different chemical reagents and easily synthesized over various particle sizes [24]. SNAzymes that functionalized with G-quadruplex DNAzymes were developed to detect various miRNA in different diseases. The abovementioned biosensors were based on chemiluminescence and electrochemiluminescence and showed excellent sensitivity [7, 18]. However, today's researches have focused on developing simple, low-cost, convenient methods like colorimetric that can detect analyte with the naked eye [25, 26]. G4 DNAzymes that are well known for their excellent peroxidase activity were used widely as a colorimetric signal transducer [27]. Among the different chromogenic substrate for peroxidase, 3,3′,5,5′-tetramethylbenzidine (TMB)-H_2O_2 system is still preferential option [25, 28].

A G-quadruplex-based SNAzyme was constructed to provide a fast and simple colorimetric method for miRNA detection. The SNAzyme is employed as both target recognition elements and catalytic nano labels for colorimetric detection. Hybridization between target miRNA and its complementary probes following the addition of target molecules led to a decrease in colorimetric signal. The proposed sensing strategy has successfully detected miRNA (miRNA-155) in spiked human serum sample with high selectivity and sensitivity. Moreover, the simple paper-based microfluidic device was developed based on SNAzyme and represented excellent results.

Experimental section

Materials and reagents

Tris or tris (hydroxymethyl) aminomethane, hemin, Tris (2-carboxyethyl) phosphine hydrochloride (TCEP), chloroauric acid ($HAuCl_4$), trisodium citrate dehydrate, sodium chloride (NaCl), potassium chloride (KCl), ethylenediaminetetraacetic acid (EDTA), 3,3′,5,5′-tetramethylbenzidine (TMB), and other chemicals were purchased from Sigma-Aldrich Chemical Co. and used without further purification. All oligonucleotide probes were synthesized from Shanghai Generay Biotech Co., Ltd. The probe sequences are listed in Table S1. Buffers and other solutions were prepared in ultrapure water.

Instrumentation

TEM analysis of bare AuNPs and functionalized AuNPs (SNAzyme) was implemented with TEM Philips EM 208S. Zeta potential was carried out on the Zetasizer Nano series (Malvern-UK). UV–Vis Spectrometer Lambda 25 (Perkin-Elmer) was used for colorimetric detection. The color intensity of paper-based assay was quantified using Image J.

Gold nanoparticle synthesis

For this synthesis, two aqueous solutions are prepared, 50 mL of chloroauric acid (1 mM) and 10 mL of trisodium citrate (38.8 mM). Chloroauric acid was heated to boiling under vigorous stirring, and then, trisodium citrate was added rapidly to the boiled-chloroauric acid solution, and continued to boil for 10 min. The solution color shows a transient color change (pale yellow to deep red) during the last minutes of synthesis [26, 29]. The AuNP solution was stored in the refrigerator at 4 °C for further application. The AuNP size based on the TEM image was about 16 nm. According to the Beer-Lambert law, using the absorption coefficient at 520 nm, the concentration of AuNPs was calculated to be about 5 nM.

Preparation of SNAzyme

Generally, AuNPs are functionalized through the salting age method, freezing directed method, and pH altering method [30, 31]. For the slating age method, initially, thiol-modified capture probe1 (100 µM, 6 µl) and thiolated G4 DNA probe (100 µM, 12 µl) were treated with freshly prepared TCEP (10 mM) for 1 h to cleave the disulfide bond. Already prepared AuNPs (1 mL) were transferred to NaOH treated glass vial, and then, the activated thiol-modified probes were added to it with gentle shaking by hand. Overnight incubation at room temperature was applied to facilitate the reaction. Furthermore, 5 µl of NaCl was added stepwise manner until the final NaCl concentration of 0.3 M and kept in RT for at least another day before use. Finally, the prepared SNAs were washed three times with TE buffer (20 min at 10,000 rpm, Eppendorf Mini spin) to remove free DNA and were redispersed in 400 µl TE buffer and stored at 4 °C for further colorimetric detection.

Detection of miRNA-155 using SNAzyme

The procedure of colorimetric detection of miRNA consists of three steps. In the beginning, SNAs (8 nM) were incubated with hemin (80 nM) for 45 min in reaction buffer (Tris–HCl 100 mM, KCl 150 mM). Before adding target

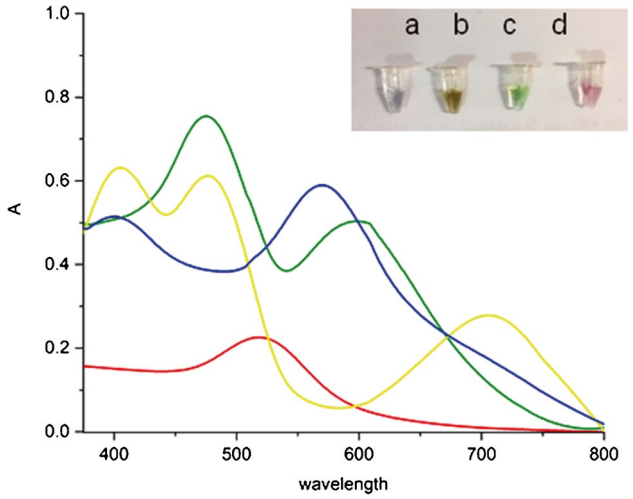

Fig. 1 Comparison of peroxidase-like activity of free **a** AuNPs (5 nM), **b** SNAzyme (5 nM), **c** hemin (80 nM), **d** functionalized AuNPs (5 nM) and in Tris buffer (100 mM, KCl 150 mM) with final volume about 200 µl

miRNA, SNAs were able to fold into the quadruplex structure and produce SNAzyme in complex with hemin. Then, the different concentration of target miRNA was added to the reaction buffer and incubated for 10 min. Moreover, capture probe 2 (50 nM) was added to the sample and targets were completely recognized. Lastly, TMB (5 µl, 100 mM) and H_2O_2 (5 µl, 1 M) were added to the solution for colorimetric measurement.

Result and discussion

Principle of miRNA-155 detection based on SNAzyme

As shown in scheme 1, we utilized G4 DNAzyme as catalytic labels to fabricate spherical nucleic acid enzyme with high peroxidase-like activity for miRNA-155 detection. To achieve this aim, first, we synthesized a spherical gold nanoparticles. Then, two DNA probes, including capture probe 1 and G-rich sequence (with a molar ratio of 1:2), were attached to already synthesized AuNPs via Au–S chemistry to create a DNA layer on the AuNPs surface. The resultant functionalized AuNPs in the optimal buffer condition (Tris–HCl 100 mM, KCl 150 mM pH 7) and presence of K^+ and hemin turn into SNAzyme. Afterward, a certain concentration of miRNA was added to the detecting

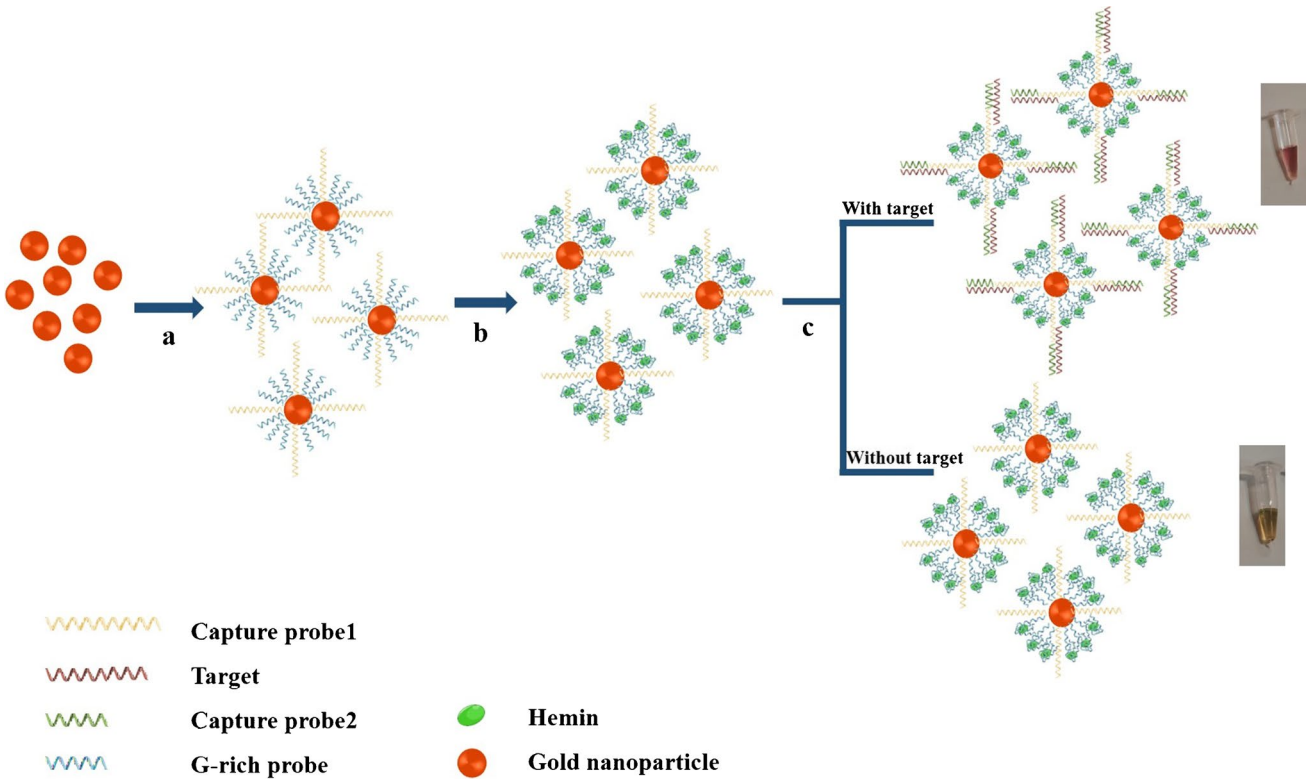

Scheme 1 Illustration of present method for colorimetric detection of miRNA-155 based on G-quadruplex SNAzymes: **a** functionalization of as-prepared AuNPs with two DNA probes (Grich DNA and capture probe 1). **b** Formation of SNAzyme in the presence of K^+ and hemin. **c** Addition of target and naked eye detection

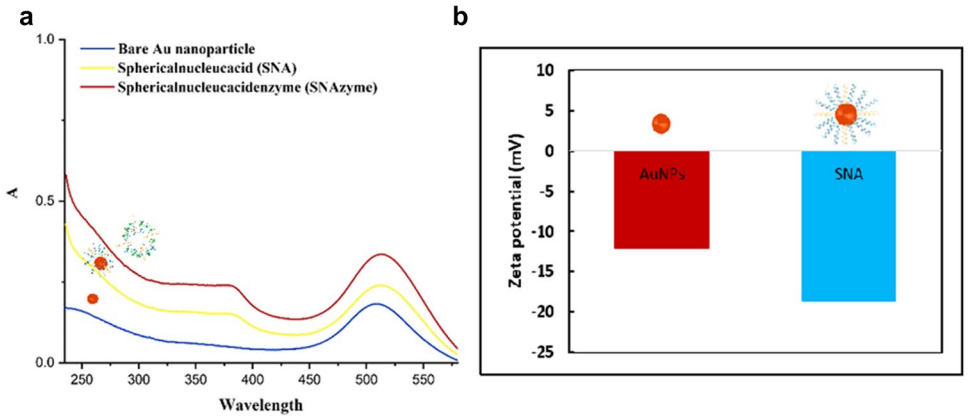

Fig. 2 **a** UV–Vis spectra for bare AuNPs (blue line), functionalized AuNPs (yellow line), SNAzyme (red line). The measurement was done in reaction buffer (Tris 100 mM, KCl 150 mM). **b** DLS analysis of zeta potential of bare AuNPs (red column) and spherical nucleic acid (blue column)

system and incubated for 5 min. Subsequently, capture probe 2 (50 nM) was added to the reaction buffer to capture the target miRNA completely. With the addition of TMB H_2O_2 as a peroxidase substrate to the reaction buffer, a weak the colorimetric response has been detected (compared to colorimetric response of the detecting system without a target). Also, the peroxidase catalytic activity of as-prepared SNAzymes was examined toward free hemin, bare AuNPs, and spherical nucleic acid under the same optimal condition. SNAzymes showed strong catalytic activity, as was to be expected (Fig. 1).

Mirkin et al. had reported that attached probes on nanoparticle surfaces show a higher binding constant to their same complementary sequence compared to free strands. On the other hand, an increase in the length of the recognition sequence leads to a decrease in binding strength [32]. So herein, we design a new colorimetric system for miRNA detection using two shorter recognition probes, DNA

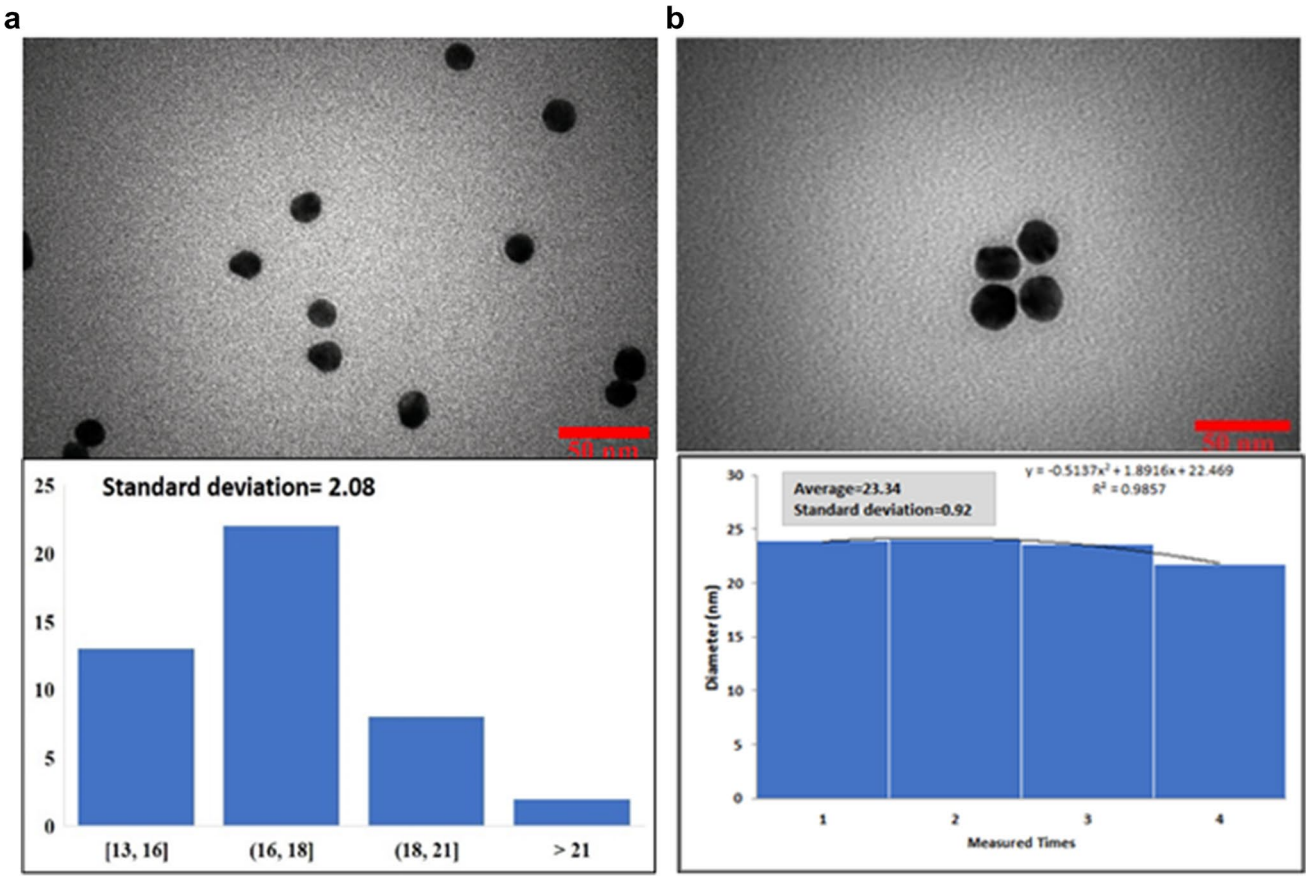

Fig. 3 TEM images and histogram of **a** bare AuNPs, **b** SNAzyme

functionalized capture probe one, and free capture probe 2. Therefore, our designed strategy has demonstrated strong and selective detection for miRNA sensing.

Characterization of SNAzyme

UV–VIS spectroscopy, TEM images, and DLS measurements provide us with detailed features of synthesized SNAzyme. Based on UV–visible data, the presence of a threshold around 260 nm for coated AuNPs compared to bare AuNps shows successful conjugation of DNA on the AuNP surface (Fig. 2a). The other method to examine the validity of SNAzyme formation is DLS data. The zeta potential results of bare AuNPs and functionalized AuNPs are shown in Fig. 2b. The functionalized AuNPs show more negative value due to the presence of aptamers than bare AuNPs. Moreover, TEM images have shown an increase in particle size after being coated with DNA, while there is no change in morphology (Fig. 3a, b).

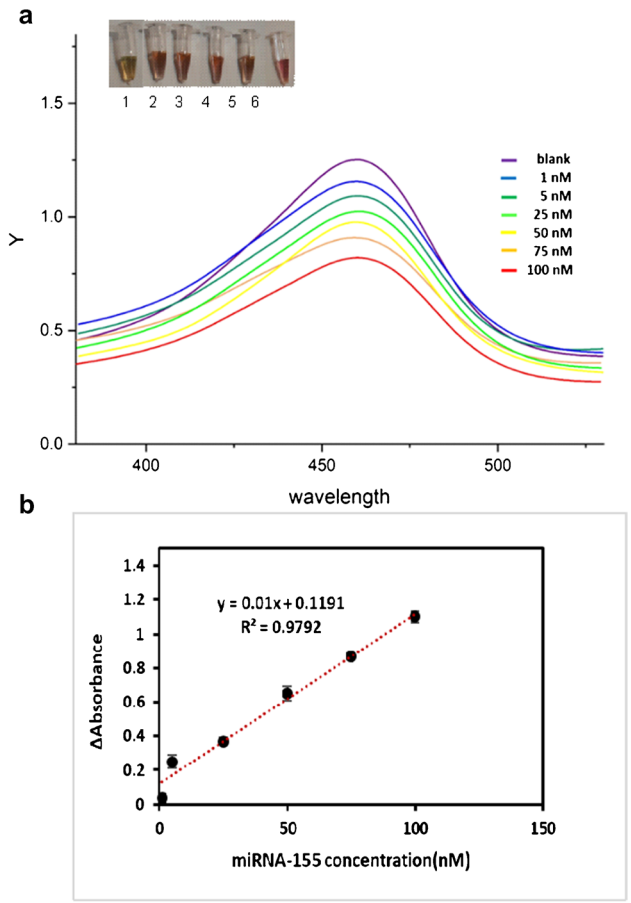

Fig. 4 **a** UV–Vis absorption spectra of SNAzyme in Tris–HCl buffer with different concentration of miRNA-155 (1 nM, 5 nM, 25 nM, 50 nM, 75 nM, 100 nM). **b** Calibration curve of miRNA-155 detection

Table 1 Comparison of present method with previous optical strategies

Method	Linear range	LOD	Reference
Fluorescence	1.02–144 nM	0.18 nM	[5]
Fluorescence	0.1–70 nM	50 pM	[6]
Fluorescence	10–2000 nM	4.2 ± nM	[7]
Colorimetric	100aM–100 fM	16.7 fM	[8]
Colorimetric	0–100 nM	16.7 fM	[9]
Colorimetric	1–100 nM	0.7 nM	This work

Optimization of effective parameters

There are several factors that can improve biosensor performance. The molar ratio between the G4 DNA probe and capture probe 1, the free complimentary probe concentration, and hemin concentration were investigated in this study. To optimize the ratio between capture probe1 and G4 DNA probe, different molar ratios were studied in terms of catalytic activity (Fig. S1). According to the results selected, the molar ratio of 2:1 (G4 DNA probe/capture probe 1) showed higher catalytic activity for the next steps.

In order to achieve the optimal concentration of free complementary probe (capture probe 2) in the reaction buffer, different concentrations of probes were examined to find out the best biosensor response. As shown in Fig. S2, 50-nm capture probe 2 exerts an apparent signal-off effect.

Since hemin shows peroxidase activity, it works as a potential factor in background signal production. To reduce the amount of noise, hemin concentration also needs to be optimized. A series of hemin concentrations was examined, and among them, the concentration 80 nM was considered as the optimal concentration for further step (Fig. S3).

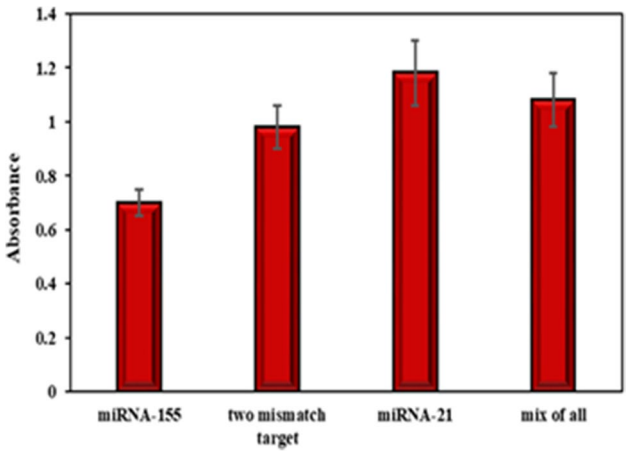

Fig. 5 Histogram of SNAzyme absorbance in the presence of target miRNA and the two other counterparts and mixture of all sequence

Table 2 Determination of miRNA-155 in human serum sample with suggested methodology

Serum sample	Added (nM)	Founded (nM)	Recovery (%)
1	12	12.27	102.25
2	25	24.2	96.8
3	50	51.5	103

The performance of colorimetric platform for miRNA-155 detection

Sensitivity of experiment

To test the response of the sensing platform toward miRNA, the colorimetric signal with increasing concentration of miRNA under optimal condition were recorded. Colorimetric response decreased with increase in the presence of the target. Steric hindrance resulting from hybridization between DNA capture probe1 and target miRNA reduces G-quadruplex access to peroxidase substrate and subsequently decreases the color change. On the other hand, the duplex between capture probes and miRNA competes with the quadruplex structure for binding to hemin. Due to these reasons, a decrease in color intensity (around 450 absorbance peak) in the presence of miRNA was observed (Fig. 4a). There is a linear relationship between colorimetric absorbance and the concentration of miRNA ranging from 1 to 100 nM ($R^2 = 0.9792$) (Fig. 4b). The method provides a low detection limit of 0.7 nM (based on 3.3 σ/S). The intercept, slope, and correlation coefficient of miRNA as determined in this work were calculated at about 0.1191 ± 0.0281, 0.01 ± 0.002, and 0.9792 ± 0.1342 ($n = 5$). According to Table 1, the analytical performance of our proposed sensing strategy was comparable with fluorescence methodologies. Furthermore, there is no need for complicated experimental steps (target amplification, separation, and washing) in our work compared to the other colorimetric methods. Compared to reported literature for miRNA detection, our colorimetric SNAzyme-based method shows a favorable sensitivity.

Selectivity

The selectivity of the biosensor was investigated for miRNA-155 toward two mismatched targets, miRNA-21, and mixtures of all sequences under the optimal conditions. As shown in Fig. 5, the experiment revealed that all these RNA counterparts have a negligible reduced effect on colorimetric absorbance compared to miRNA-155, so this simple and efficient colorimetric system can be considered a selective method for miRNA-155 detection.

miRNA detection in spiked sample

To evaluate the applicability of the assay, various concentrations of miRNA-155 were spiked in diluted human serum (1:100 ratio). The pre-treatment includes thawing the frozen plasma to reach the room temperature and diluted the plasma with phosphate buffer before spike. As shown in Table 2, recoveries are from 96.8 to 103%. The result indicates good accuracy for miRNA detection in a real biological sample.

Paper-based assay

The paper-based microfluidic device is an ideal candidate for developing point-of-care diagnostic tests [33]. To evaluate the operation of the proposed biosensor in microfluidic devices, the initial stages of the simple paper test were also performed and showed successful results. The Whatman filter No.1 was applied for the paper-based tests, and PVC sheets were employed to avoid leakage from the spot zone. To examine the catalytic activity of the sensor, 3 µl of SNAzyme, hemin, and AuNPs was loaded to different spot zones and let it dry for a few minutes. After that, 3 µl of TMB and H_2O_2 was added to each spot zone, and a short time later, the

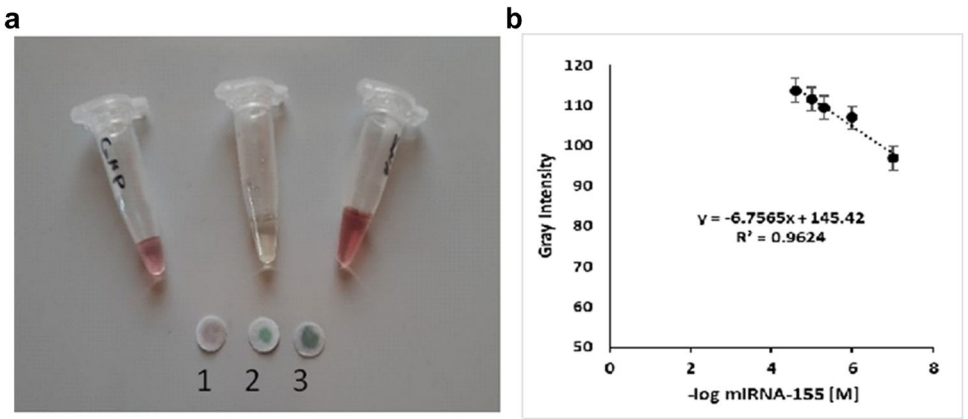

Fig. 6 **a** Three different paper-based detection zone loading with (1) 3 µl of bare AuNPs + 2 µl TMB (100 mM) + 2 µl of H_2O_2 1 M. (2) 3 µl of hemin + 2 µl TMB (100 mM) + 2 µl of H_2O_2 1 M. (3) 3 µl of SNAzyme + 2 µl TMB (100 mM) + 2 µl of H_2O_2 1 M. **b** The linear relationship between different miRNA-155 concentration and gray intensity

color change was observed (Fig. 6a). The taken photos from the zone were quantified with Image J for precise measurement. Moreover, the performance of the biosensor toward different concentrations of target miRNA-155 was tested. Based on the result, the gray intensity gradually increased with increasing miRNA-155 concentration, and the calibration curve exhibited the linear relationship between gray intensities and miRNA concentration (0.1 µM, 1 µM, 5 µM, 10 µM, 20 µM) (Fig. 6b).

Conclusion

In summary, a novel and sensitive colorimetric strategy has been developed based on SNAzyme for miRNA detection. The strategy relies on a decrease in color intensity resulting from duplex formation between capture probes and miRNA. G-quadruplex DNAzymes were used as Nano labels to produce a colorimetric response. Briefly, target miRNA was detected by hybridization between two capture probes including capture probe1 located on the AuNPs' surface and free capture probe 2. This leads to a decrease in peroxidase-like activity of DNAzyme and colorimetric response. Via this method, the linear response range from 1 to 100 nM was reported. To investigate the further application of the proposed method, a simple paper test was also done, and good results were achieved. Utilizing amplification techniques coupled with this detection system may develop more sensitive the colorimetric biosensors. The performance of colorimetric assay was also demonstrated on a paper-based microfluidic device.

Supplementary Information The online version contains supplementary material available at https://doi.org/10.1007/s00604-022-05455-7.

Acknowledgements The authors are grateful to the Research Council of University of Tehran for the financial support of this work.

Author contribution Kosar Shahsavar: conceptualization, methodology, writing—original draft; Morteza Hosseini: resources, supervision, funding acquisition, and review and editing; Ehsan Shokri: validation, writing—review and editing.

Declarations

Competing interest The authors declare no competing interests.

References

1. Borghei YS, Hosseini M, Dadmehr M, Hosseinkhani S, Ganjali MR, Sheikhnejad R (2016) Visual detection of cancer cells by colorimetric aptasensor based on aggregation of gold nanoparticles induced by DNA hybridization. Anal Chim Acta 904:92–97. https://doi.org/10.1016/j.aca.2015.11.026
2. Condrat CE, Thompson DC, Barbu MG, Bugnar OL, Boboc A, Cretoiu D, Suciu N, Cretoiu SM, Voinea SC (2020) miRNAs as biomarkers in disease: latest findings regarding their role in diagnosis and prognosis. Cells 9(2):276. https://doi.org/10.3390/cells9020276
3. Wang H, Peng R, Wang J, Qin Z, Xue L (2018) Circulating microRNAs as potential cancer biomarkers: the advantage and disadvantage. Clin Epigenetics 10:59. https://doi.org/10.1186/s13148-018-0492-1
4. Ying L, Du L, Zou R, Shi L, Zhang N, Jin J, Xu C, Zhang F, Zhu C, Wu J, Chen K, Huang M, Wu Y, Zhang Y, Zheng W, Pan X, Chen B, Lin A, Tam JKC, van Dam RM, Lai DTM, Chia KS, Zhou L, Too HP, Yu H, Mao W, Su D (2020) Development of a serum miRNA panel for detection of early stage non-small cell lung cancer. Proc Natl Acad Sci U S A 117(40):25036–25042. https://doi.org/10.1073/pnas.2006212117
5. Shahsavar K, Shokri E, Hosseini M (2020) A fluorescence-readout method for miRNA-155 detection with double-hairpin molecular beacon based on quadruplex DNA structure. Microchem J 158:105277. https://doi.org/10.1016/j.microc.2020.105277
6. Nemati F, Hosseini M (2021) A ratiometric fluorescence and colorimetric dual-mode assay for miRNA-155 based on Ce-decorated boron nitride nanosheets. Microchem J 168:106346. https://doi.org/10.1016/j.microc.2021.106346
7. Bian F, Sun L, Cai L, Wang Y, Zhao Y, Wang S, Zhou M (2019) Molybdenum disulfide-integrated photonic barcodes for tumor markers screening. Biosens Bioelectron 133:199–204. https://doi.org/10.1016/j.bios.2019.02.066
8. Wang L, Liu Z-J, Cao H-X, Liang G-X (2021) Ultrasensitive colorimetric miRNA detection based on magnetic 3D DNA walker and unmodified AuNPs. Sens Actuators, B Chem 337:129813. https://doi.org/10.1016/j.snb.2021.129813
9. Lee J, Kim Y-k, Lee S, Yoon S, Kim W-k (2019) Graphene oxide-based NET strategy for enhanced colorimetric sensing of miRNA. Sens Actuators, B Chem 282:861–867. https://doi.org/10.1016/j.snb.2018.11.149
10. Kong W, He L, Richards EJ, Challa S, Xu CX, Permuth-Wey J, Lancaster JM, Coppola D, Sellers TA, Djeu JY, Cheng JQ (2014) Upregulation of miRNA-155 promotes tumour angiogenesis by targeting VHL and is associated with poor prognosis and triple-negative breast cancer. Oncogene 33(6):679–689. https://doi.org/10.1038/onc.2012.636
11. Gurses HE, Hatipoğlu OF, Gunduz M, Gunduz E (2015) MicroRNAs as therapeutic targets in human breast cancer. In: Gunduz M (ed) A concise review of molecular pathology of breast cancer, Chapter 5. InTech, Croatia, pp 121–137. https://doi.org/10.5772/59681
12. Gillespie P, Ladame S, O'Hare D (2018) Molecular methods in electrochemical microRNA detection. Analyst 144(1):114–129. https://doi.org/10.1039/c8an01572d
13. Ye J, Xu M, Tian X, Cai S, Zeng S (2019) Research advances in the detection of miRNA. J Pharm Anal 9(4):217–226. https://doi.org/10.1016/j.jpha.2019.05.004
14. Wan Z, Umer M, Lobino M, Thiel D, Nguyen N-T, Trinchi A, Shiddiky MJA, Gao Y, Li Q (2020) Laser induced self-N-doped porous graphene as an electrochemical biosensor for femtomolar miRNA detection. Carbon 163:385–394. https://doi.org/10.1016/j.carbon.2020.03.043
15. Huang R, Liao Y, Zhou X, Fu Y, Xing D (2017) Multiplexed detection of microRNA biomarkers from tumor cells and tissues with a homogeneous nano-photon switch. Sens Actuators, B Chem 247:505–513. https://doi.org/10.1016/j.snb.2017.03.055
16. Fiammengo R (2017) Can nanotechnology improve cancer diagnosis through miRNA detection? Biomark Med 11(1):69–86. https://doi.org/10.2217/bmm-2016-0195

17. Cutler JI, Auyeung E, Mirkin CA (2012) Spherical nucleic acids. J Am Chem Soc 134(3):1376–1391. https://doi.org/10.1021/ja209351u
18. Sun Y, Shi L, Wang Q, Mi L, Li T (2019) Spherical nucleic acid enzyme (SNAzyme) boosted chemiluminescence miRNA imaging using a smartphone. Anal Chem 91(5):3652–3658. https://doi.org/10.1021/acs.analchem.8b05696
19. Sun Y, Wang Q, Mi L, Shi L, Li T (2019) Target-induced payload amplification for spherical nucleic acid enzyme (SNAzyme)-catalyzed electrochemiluminescence detection of circulating microRNAs. Anal Chem 91(20):12948–12953. https://doi.org/10.1021/acs.analchem.9b03001
20. Mirkin CA, Letsinger RL, Mucic RC, Storhoff JJ (1996) A DNA-based method for rationally assembling nanoparticles into macroscopic materials. Nature 382(6592):607–609. https://doi.org/10.1038/382607a0
21. Li Z, Jin R, Mirkin CA, Letsinger RL (2002) Multiple thiol-anchor capped DNA-gold nanoparticle conjugates. Nucleic Acids Res 30(7):1558–1562. https://doi.org/10.1093/nar/30.7.1558
22. Sato K, Hosokawa K, Maeda M (2003) Rapid aggregation of gold nanoparticles induced by non-cross-linking DNA hybridization. J Am Chem Soc 125(27):8102–8103. https://doi.org/10.1021/ja034876s
23. Karami A, Hasani M, Azizi Jalilian F, Ezati R (2021) Conventional PCR assisted single-component assembly of spherical nucleic acids for simple colorimetric detection of SARS-CoV-2. Sens Actuators B Chem 328:128971. https://doi.org/10.1016/j.snb.2020.128971
24. Frens G (1973) Controlled nucleation for the regulation of the particle size in monodisperse gold suspensions. Nat Phys Sci 241(105):20–22. https://doi.org/10.1038/physci241020a0
25. Shahsavar K, Hosseini M, Shokri E, Ganjali MR, Ju H (2017) A sensitive colorimetric aptasensor with a triple-helix molecular switch based on peroxidase-like activity of a DNAzyme for ATP detection. Anal Methods 9(32):4726–4731. https://doi.org/10.1039/c7ay01381g
26. Naderi M, Hosseini M, Ganjali MR (2018) Naked-eye detection of potassium ions in a novel gold nanoparticle aggregation-based aptasensor. Spectrochim Acta A Mol Biomol Spectrosc 195:75–83. https://doi.org/10.1016/j.saa.2018.01.051
27. Shahsavar K, Hosseini M, Shokri E, Xu G (2021) New insight into G-quadruplexes; diagnosis application in cancer. Anal Biochem 620:114149. https://doi.org/10.1016/j.ab.2021.114149
28. Dehghani Z, Hosseini M, Mohammadnejad J, Bakhshi B, Rezayan AH (2018) Colorimetric aptasensor for Campylobacter jejuni cells by exploiting the peroxidase like activity of Au@Pd nanoparticles. Mikrochim Acta 185(10):448. https://doi.org/10.1007/s00604-018-2976-2
29. Hosseini M, Khabbaz H, Dadmehr M, Ganjali MR, Mohamadnejad J (2015) Aptamer-based colorimetric and chemiluminescence detection of aflatoxin B1 in foods samples. Acta Chim Slov 62(3):721–728. https://doi.org/10.17344/acsi.2015.1358
30. Liu J, Lu Y (2006) Preparation of aptamer-linked gold nanoparticle purple aggregates for colorimetric sensing of analytes. Nat Protoc 1(1):246–252. https://doi.org/10.1038/nprot.2006.38
31. Liu B, Liu J (2017) Freezing directed construction of bio/nano interfaces: reagentless conjugation, denser spherical nucleic acids, and better nanoflares. J Am Chem Soc 139(28):9471–9474. https://doi.org/10.1021/jacs.7b04885
32. Lytton-Jean AK, Mirkin CA (2005) A thermodynamic investigation into the binding properties of DNA functionalized gold nanoparticle probes and molecular fluorophore probes. J Am Chem Soc 127(37):12754–12755. https://doi.org/10.1021/ja052255o
33. Shah P, Zhu X, Li CZ (2013) Development of paper-based analytical kit for point-of-care testing. Expert Rev Mol Diagn 13(1):83–91. https://doi.org/10.1586/erm.12.130